Spring 5-1-2015

Outer-sphere adsorption of para-substituted benzoates on gibbsite: a molecular dynamics investigation

Lukas McNaboe
luke.mcnaboe@gmail.com

University of Connecticut

Senior Honors Thesis

Outer-sphere adsorption of para-substituted benzoates on gibbsite: a molecular dynamics investigation

Author:
Luke McNaboe

Advisor:
Dr. Chad Johnston

A thesis submitted in fulfillment of the requirements for the degree of Environmental Engineering

in the

Department of Civil and Environmental Engineering

May 13, 2015

Abstract

In soils, the spread of toxic organic anions through groundwater can be partially mitigated by the formation of inner- and outer-sphere complexes with aluminum (hydr)oxides. In current practice, a constant soil-water partition coefficient is used to describe the relative quantity of sorbed compound to that in solution. However this method is empirical and site-specific. In order to establish a thermodynamically relevant sorption model, sorption reactions between many mineral phases and organic compounds must be characterized. While there exists a wealth of research quantifying the sorption potential of ferric oxide mineral phases, there remains a gap in knowledge of these parameters for aluminum oxides. In this study, the energy of outer-sphere complexation reactions will be calculated based on electrostatic and van der Waals interactions between gibbsite ($Al(OH)_3$) and the benzoate compounds using LAMMPS molecular dynamics software. To achieve this objective, adsorption energies have been calculated for benzoate ions with the follwing para-substituted functional groups: nitro-, chloro-, methoxy-, methyl-, and amine-. This research is an advancement of an ongoing effort to develop a thermodynamically relevant adsorption model.

1 Introduction

The transport and fate of toxic elements in the lithosphere is largely dependent on adsorption reactions at the surfaces of metal hydroxides [1][2]. Accurately predicting the impact of soil contamination entails understanding the formation of these complexes at a molecular level. Current predictive contaminant transport models [3] fail to account for outer-sphere complexation reactions governed by electrostatic and Van der Waals forces at the surface, thereby underestimating the magnitude of sorption.

Molecular dynamics (MD) simulations such as LAMMPS [4] generate robust models of complex atomic-level processes. The free energy of outer-sphere surface complexation (ΔG_{sorb}) can be predicted by measuring the change in mean force potential (PMF) as a sorbate is forced closer to a surface [5]. A windowed-umbrella sampling procedure [6] can be used to collect this data. The difference between long-range and minimum energy levels was taken to be ΔG_{sorb} [22] for outer-sphere surface complexation.

Outer-sphere sorption is also dependent on sorbate-specific properties such as size and binding-site electron density. Trajectory data and an accurate depiction of the surface's electrostatic potential can be used to understand these electrostatic interactions [7][8]. In order to investigate these sorbate-specific effects, adsorption energies have been calculated for benzoate ions with the following para-substituted functional groups: nitro-, chloro-, methoxy-, methyl-, and amine-. Benzoate was selected as the base structure for the adsorption experiments for two reasons. First, its negatively-charged carboxylate

group is a key structural moiety in outer-sphere surface complexation reactions [9] and therefore serves as an appropriate probe compound in the study of these reactions. Secondly, the benzene ring is a relatively apolar component that serves to slightly mitigate the steric and electron-withdrawing effects of groups substituted onto the opposite end of the molecule. A comparison of the relative adsorption potentials and trajectory data for these compounds will develop understanding of structural effects on outer-sphere surface complexation.

Gibbsite is one of the most abundant forms of aluminum hydroxide in the dynamic supergene environment. While its basal (001) plane is more abundant [10], its edge (100) face is more reactive in sorption interactions [11][12] due to (i) the lower free energy of edge-bound -OH groups and (ii) the more accessible pK_a values on this face.

This research will quantify the favorability of outer-sphere surface complexation reactions between gibbsite and the aforementioned sorbate molecules in order to advance the ongoing effort of developing a robust, thermodynamically relevant sorption model.

2 Methods

Molecular dynamics simulations were run using LAMMPS [4], a classical MD program capable of modeling large systems of particles with user-defined thermodynamic and boundary conditions as well as comprehensive force field parameters.

The previously reported structure of gibbsite [13] with a unit cell formula of $Al_8(OH)_{24}{\cdot}4H_2O$ was used in the creation of a simulation model. Water molecules were included in order to satisfy surficial Al^{3+} bonding. Two super cells were created to study adsorption on edge (100) and basal (001) faces in order to comprehensively investigate the mineral's sorption potential. The edge face was constructed by translating the unit cell two times in the x and z dimensions and four times in the y dimension ($2 \times 4 \times 2$) for a total of 16 unit cells. The resulting super cell had dimensions of 17.4 Å $\times$ 20.3 Å $\times$ 19.5 Å and a total of four slabs. A visualization of a basal slab is shown in figure 1. As the yz plane corresponded to the more capricious (100) face of gibbsite [12], these y and z dimensions

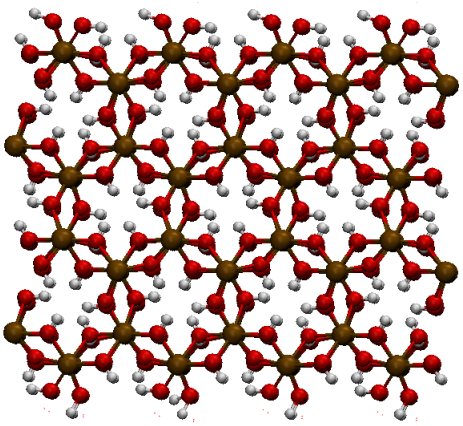

Figure 1: View of the xy plane (001) of the gibbsite crystal

were used to create a periodic simulation box with a final size of 56.2 Å × 20.3 Å × 19.5 Å. The basal super cell was constructed by translating the unit cell along the dimension (4 × 4 × 2), yielding a total of 3 slabs of gibbsite. These boxes were then filled with water molecules to reach a density of 1.0 g/cm^3. Gibbsite was modeled using parameters derived in the CLAYFF force field [14]; the bending and stretching parameters for water were defined according to the simple point-charge (SPC) model [15].

The geometry and partial charges of the organic anion solute molecules were determined using the program Gaussian 09[28] and the RESP[29] method, respectively. The set of experimental compounds are shown in figure 2. The para-substituted functional groups were selected due to their varying electronegativity and molecular weight.

The system's topological information was compiled into a data file (examples included in appendix) which was read into a LAMMPS input script. The total energy of the simulation was determined by evaluating the energy term for either bonded or non-bonded interactions. Non-bonded interactions consisted of Coulombic (electrostatic) and Van der Waals interactions; these were evaluated for each atom pair according to equation 1, where the first summation term accounts for electrostatic energy and the second accounts for VdW energy.

$$E_{non-bond,ij} = \frac{e^2}{4\pi\epsilon_0}\sum_{i\neq j}\frac{q_i q_j}{r_{ij}} + \sum_{i\neq j} D_{o,ij}\left[\left(\frac{R_{o,ij}}{r_{ij}}\right)^{12} - 2\left(\frac{R_{o,ij}}{r_{ij}}\right)^{6}\right] \quad (1)$$

The energy is inversely proportional to the distance r_{ij} between 2 atoms. This energy is ramped smoothly to zero between 9 and 10 Å which eliminates noise from a more abrupt cutoff. The e term refers to the charge of an electron and ϵ_0 is the dielectric permittivity of free space. D_o and R_o are empirical parameters derived in the development of the CLAYFF [14] model of hydroxide soil phases. The energy between bonded atoms includes

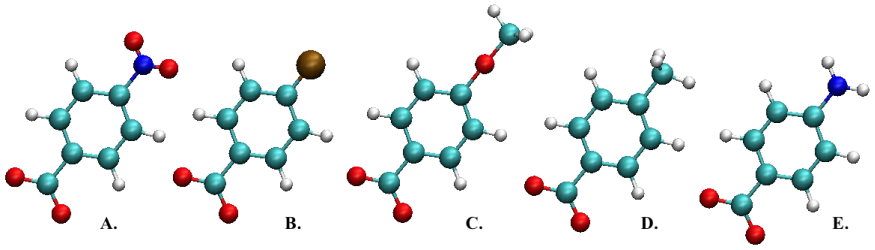

Figure 2: The organic anion compounds used as sorbate compounds in the experiment. From left to right, shown are A. Nitro- B. Chloro- C. Methoxy- D. Methyl- and E. Aminobenzoate. *Note: Scale between figures is not constant.*

bond stretch, angle bend, dihedral torsion, and improper energy terms that are accounted for in (a) the CLAY force field for the mineral, (b) the SPC model [15] for water and (c) the generalized AMBER force field (GAFF) [16] for sorbate molecules. The energy terms for bonded atoms are enumerated in equation 2.

$$E_{bond} = k_{stretch}(r_{ij} - r_0)^2 + k_{bend}(\theta_{ijk} - \theta_{0,ijk})^2 + k_{torsion}[1 + cos(n\phi - d)] + k_{imp.}[1 + dcos(n\phi)] \quad (2)$$

In each of these terms, the k constant is an energy parameter, r_0 and θ_0 are equilibrium bond length and angle parameters, and d and n are integer values specific to either torsional or improper interactions. These constant values were obtained from the three force field models listed above.

LAMMPS calculates the positions and velocities of each atom using a time integration of Nose-Hoover equations of motion. The system was set to equilibrate in a canonical ensemble (*nvt*: constant number of particles, volume, temperature) at a time step of 0.1 fs, for 10 ps. The average temperature was set to 300.0 K. The liquid phase was set to equilibrate in an isobaric-isothermal (*npt*) ensemble, in which the pressure was held constant at 1.0 atm for an additional 10 ps, for a total of 20 ps. As shown in figure 3, the

Van der Waals energy reached an equilibrium energy level after 2 ps and the coulombic (electrostatic) energy completely equilibrated after 6 ps.

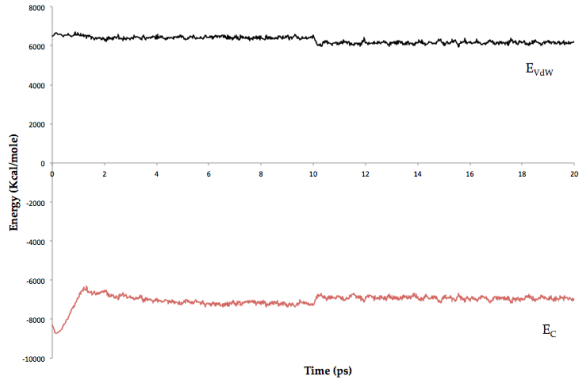

Figure 3: System equilibration over a period of 20 ps. After the first 10 ps, the system switches from *nvt* to *npt*.

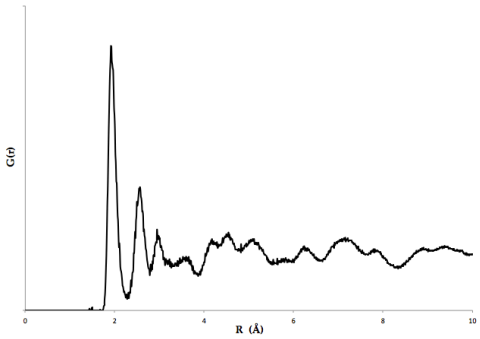

Figure 4: Pair distribution function of gibbsite.

After 10ps, a slight shift in energy was observed as the system changed from *nvt* to *npt*. However this change did not result in a prolonged loss of equilibrium. This equilibrium thermodynamic state (20 ps) was taken as the initial condition in further analysis.

Radial pair distribution functions were calculated with the tool included with VMD [17]. As shown in figure 4, the rdf G(r) was computed for all atoms around Al^{3+}. The peak locations are in good agreement with EXAFS measurements of gibbsite [18] as well as other simulated radial distributions [19]. The first peak ($R = 1.9\mathring{A}$) corresponds to Al-O bonds and the following two peaks correspond to Al-H and Al-Al distances, respectively.

The output of umbrella sampling (a PMF curve) is equivalent to the free energy profile [5] as it records the change in total system energy as a function of distance.

Free energy profiles were generated by fixing the centers of mass of the sorbate and gibbsite at a certain separation distance according to a spring function. This spring function had a corresponding force constant (k, Kcal/mole) which was set to 10 for all distances $x > 3$Å. The initial separation distance $x_i = 20\mathring{A}$ between centers of mass was large enough so that the surface's electrostatic and Van der Waals effects were negligible. As shown in figure 5, these effects end at a surface separation distance (SSD) of approximately 7 Å, which is approximately 16 Å from the mineral's center of mass. The

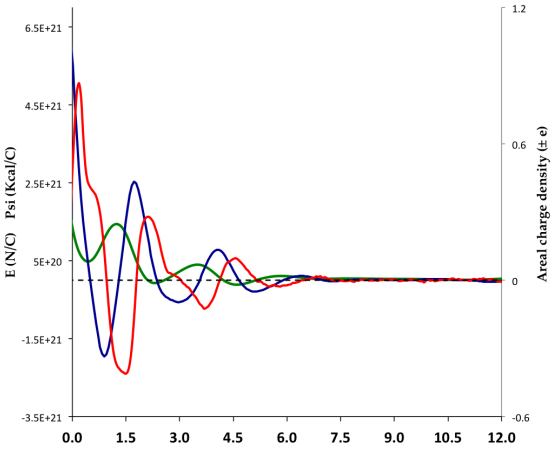

Figure 5: Surface effects on charge (red), electric field (blue), and electrostatic potential (green) for edge (100) surface.

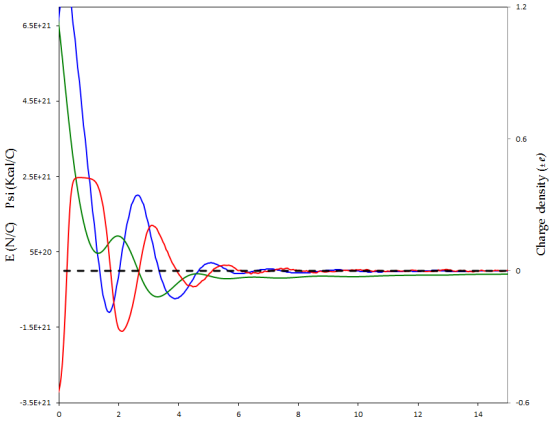

Figure 6: Surface effects on charge (red), electric field (blue), and electrostatic potential (green) for basal (001) surface.

coordinate of the mineral surface was fixed based on this data and trajectory data from the MD simulations. During window-umbrella sampling, the sorbate was initially held at x_i and subsequent distances x (where $dx = 0.5$Å) for 500 ps each. The final x was such that the sorbate's center of mass was to be held at the surface (i.e. SSD = 0); this range fully encompasses the range at which outer-sphere surface complexation may occur.

3 Discussion of Results

Sorbate compounds were initially fixed 12 Å from the surface, and forced downward by 0.5 Å every 500 ps. Features of the measured free energy along this path are attributed to (a) electrostatic effects of the regimented gibbsite surface, (b) charge distribution within the sorbate compound, and (c) mass distribution of the sorbate compound.

As both mineral surfaces have a net positive charge (figures 5, 6) a specific arrangement of water molecules was observed beginning at approximately 1Å from the surface. This accumulation has also been seen in simulations involving goethite [31]. The structured orientation of the water molecules generates a distinct oscillation between excess positive and negative charges; this gradually diminishes to a neutral charge as the structure's effects become less influential when further from the surface. Many models of the

electric structures of mineral surfaces have been proposed [33] [32], predicting an electric double or triple layer. Observations from this model of the primary gibbsite surfaces correspond with the work of Kerisit *et al.* in that several condensed layers could be observed in the net charge away from the surface. Additionally, the edge (100) surface had three distinct negative electric fields, whereas only two were observed on the basal (001) surface. Not only can these surface-dependent features affect the ΔG_{sorb} [31] as discussed below, but they also indicate that a general model of surface charge distribution may be inaccurate [30] due to its inherent dependence on the mineral's molecular structure.

Outer-sphere adsorption for each anion on both surfaces of gibbsite is favorable. Beginning at a SSD of 12 Å and moving toward the surface, each compound gradually experiences a favorable change (decrease) in free energy. The minimum energy occurs between 5.50-7.50 Å from the edge surface, and at a distance of 4.80-5.80Å from the basal surface; these ranges of minimums correspond to a slightly positive electric field generated by the surface, as shown in figs. 5 6. Additionally, the anionic moieties are attracted to the positively charged surface. A negatively charged electric field slightly repels the anion from this sampling window and therefore the free energy in this range required aggressive sampling. Initially, the energy for this range was assumed to be orders of magnitude higher than the surrounding energy levels. Further investigation of this negative electric field region with all five compounds involved (i) decreasing the sampling interval dx to 0.25Å and (ii) increasing the force constant to 50. This intensive sampling procedure kept the sorbate in narrow intervals; each interval corresponds with a peak free energy level. These peaks are within 0.5Å of each other, indicating a largely constant free energy level for this range. As the sorbate anions are forced to distances $x < 4$Å, the free energy increases to overcome the increasing electrostatic potential. Any subsequent decreases in ψ corresponds to a slight $-\Delta G$, but measured free energy values for $x < 4$Å are consistently greater than the constant energy value found far from the surface, indicating unfavorable outer-sphere surface complexation at these close distances. On the basal face, the electrostatic potential was gentler such that the compounds were permitted to reach closer to the surface, and an estimation of inner sphere sorption free energy can be

interpreted from the minimum found at approximately 2.25Å.

As shown in table 1, p-Chloro-, -Nitro-, and -Methoxybenzoate yield the least favorable sorption potentials on the edge face. This may initially be attributed to their comparably high molecular weights, but further analysis reveals that other factors are also influential. When running window-umbrella sampling for these solutes, the electrostatic solute-surface interactions cause a disintegration of the surface at $x = 2$ and 2.5Å for chloro- and p-Nitrobenzoate, respectively. The chloro- anion can reach slightly closer to the surface due to its lower molecular weight. The even lighter methoxy- anion can complete the run without breaking surficial bonds, however it generates a less favorable ΔG than the nitro- anion due to the greater charge distribution about the methoxy-functional group.

A higher charge density in the carboxylate group can encourage greater attraction to the positively charged surface features; this is manifested as a minimum PMF coordinate slightly closer to the surface.

On the basal (001) face, outer sphere surface complexation was also found to be favorable, but the free energy data in table 1 indicates that it is slightly less so than on the edge face (i.e. greater ΔG_{sorb}). This is likely a result of the surface-bound hydroxides having pK_a values outside of the natural environment.

Table 1: A summary of minimum free energy data for each sorbate anion on both major faces of gibbsite. Shown are the magnitudes of each anion's minimum energy (Kcal/mole) and the location of these minimums with respect to the surface (Å). The right column shows the carboxylate group's net partial charge, in units of e. The data for the p-Nitrobenzoate interaction on 001 was not obtained due to scripting error.

001 Basal			100 Edge		
PMF_{min}	SSD_{min}	p-Group	PMF_{min}	SSD_{min}	Q_{COO^-}
-1.89	4.82	$-CH_3$	-9.26	5.50	-0.887
-0.84	4.91	$-NH_2$	-5.71	5.74	-0.794
N/A	N/A	$-NO_2$	-4.78	6.94	-0.776
-1.35	5.72	$-OCH_3$	-4.03	7.42	-0.774
-1.15	5.18	-Cl	-3.99	5.62	-0.789

These PMF_{min} values represent predicted ΔG_{sorb} parameters required in the formu-

lation of thermodynamically meaningful adsorption stoichiometry.

4 Conclusion

The purpose of this research was to investigate and quantify the potential for organic anions to form outer-sphere surface complexes with gibbsite. The free energy for these interactions was found to be negative, indicating that this is a thermodynamically favorable process. In addition, the free energy of sorption was predicted for these interactions, which can be used to account for this sorption mechanism in robust contaminant transport models.

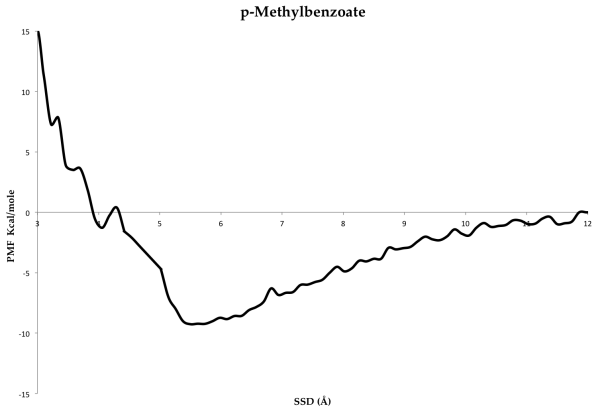

Figure 7: Free energy profile: p-Methoxybenzoate adsorbed onto 100 edge face of gibbsite.

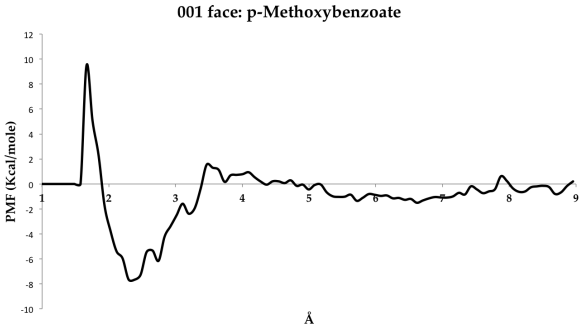

Figure 8: Free energy profile: p-Methoxybenzoate adsorbed onto 001 edge face of gibbsite.

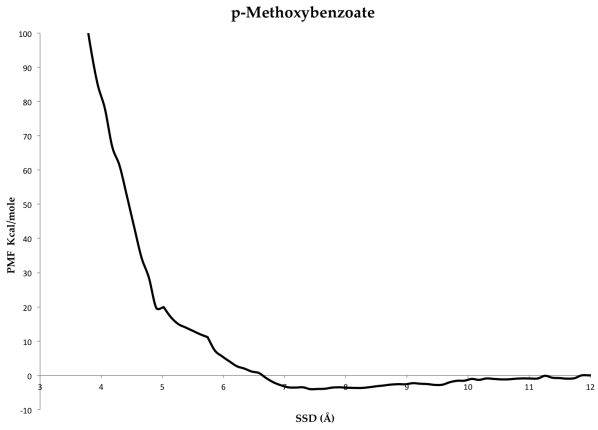

Figure 9: Free energy profile: p-Methylbenzoate adsorbed onto 100 edge face of gibbsite.

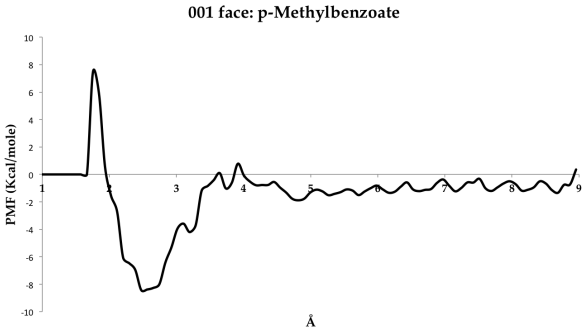

Figure 10: Free energy profile: p-Methylbenzoate adsorbed onto 001 edge face of gibbsite.

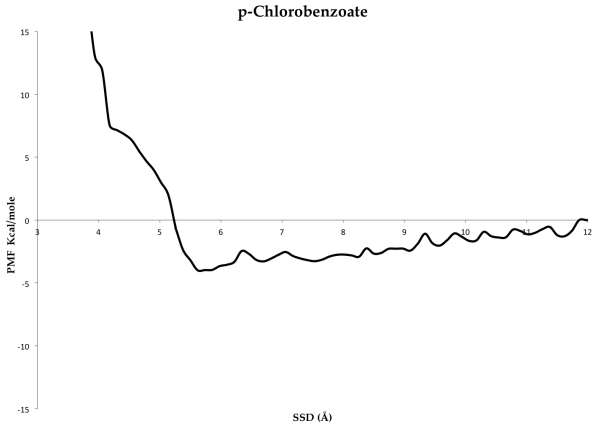

Figure 11: Free energy profile: p-Chlorobenzoate adsorbed onto 100 edge face of gibbsite.

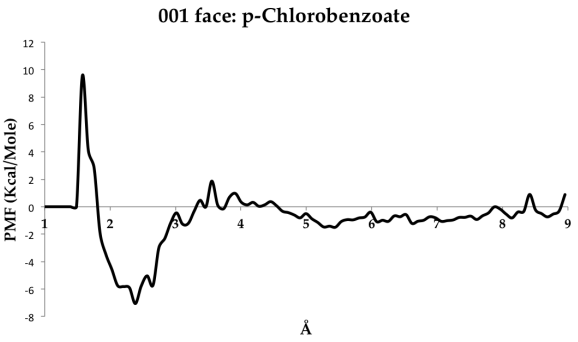

Figure 12: Free energy profile: p-Chlorobenzoate adsorbed onto 001 edge face of gibbsite.

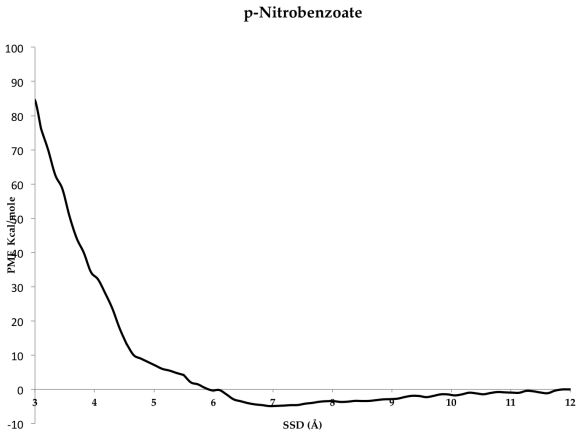

Figure 13: Free energy profile: p-Nitrobenzoate adsorbed onto 100 edge face of gibbsite.

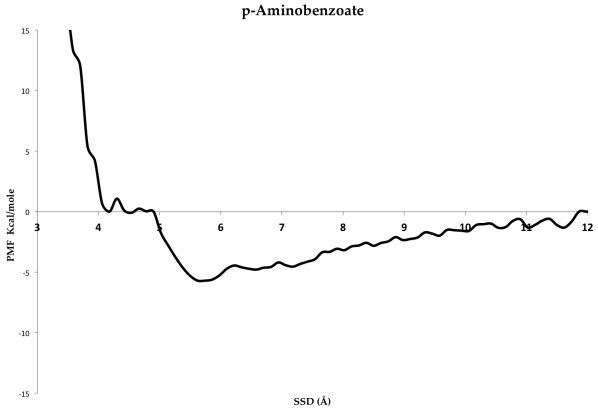

Figure 14: Free energy profile: p-Aminobenzoate adsorbed onto 100 edge face of gibbsite.

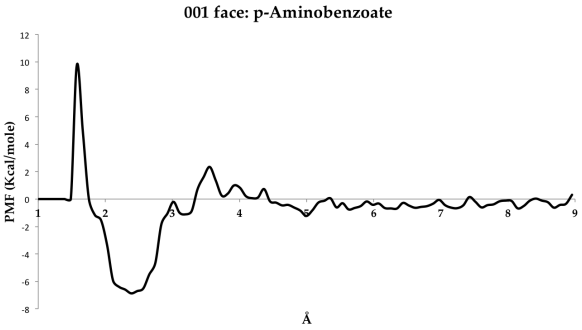

Figure 15: Free energy profile: p-Aminobenzoate adsorbed onto 001 edge face of gibbsite.

References

[1] Ertl, G.; Knoezinger, H.; et al. Environmental Catalysis. Wiley-VCH, 1999.

[2] Ladiera, A.; Ciminelli, V.; et al. Mechanism of anion retention from EXAFS and density functional calculations: Arsenic (V) adsorbed on Gibbsite. *Geochimica et Cosmochimica Acta.* 65(8):1211-1217, 2001.

[3] *Estimation Programs Interface Suite for Microsoft Windows (EPISuite)*, version 4.11; US Environmental Protection Agency: Washington, DC, 2012.

[4] Plimpton, S. Fast Parallel Algorithms for Short-Range Molecular Dynamics. *Journal of Computational Physics* 117:1-19, 1995.

[5] Kumar, S.; Rosenberg, J.; et al. The Weighted Histogram Analysis Method for Free Energy Calculations on Bio-molecules. I: the method. *Journal of Computational Chemistry* 13(8):1011-1021, 1992.

[6] Wang, F.; Stuart, S.; et al. Calculation of adsorption free energy for solute-surface interactions using biased replica-exchange molecular dynamics. *Biointerphases* 3(9), 2008.

[7] Teppen, B.; Rasmussen, K.; et al. Molecular Dynamics Modeling of Clay Minerals. 1. Gibbsite, Kaolinite, Pyrophyllite, and Beidellite. *Journal of Physical Chemistry, B* 101:1579-1597, 1997.

[8] Strongin, D.; Grey, C.; et al. Surface science studies of environmentally relevant iron (oxy)hydroxides ranging from the nano to the macro-regime. *Surface Science* 604:1065-1071, 2010.

[9] MacKay, A.; Vasudevan, D. Polyfunctional Ionogenic Compound Sorption: Challenges and New Approches To Advance Predictive Models. *Environmental Science and Technology* 46:9209-9233, 2012.

[10] Rosenqvist, J.; Axe, K.; et al. Adsorption of dicarboxylates on nano-sized gibbsite particles: effects of ligand structure on bonding mechanisms. *Colloids and Surfaces A: Physicochemical Engineering Aspects* 220:91-104, 2003.

[11] Sposito, G. The Surface Chemistry of Soils. *Oxford University Press*, New York, 1984

[12] Liu, X.; Cheng, J.; et al. Understanding surface acidity of gibbsite with first principles molecular dynamics simulations. *Geochimica et Cosmochimica Acta* 120:487-495, 2013.

[13] Saalfeld, H.; Wedde, M. Refinement of the crystal structure of gibbsite, $Al(OH)_3$. *Zeitschrift für Kristallographie* 139(1-6):129-135, 1974.

[14] Cygan, R.; Liang, J.; et al. Molecular Models of Hydroxide, Oxyhydroxide, and Clay Phases and the Development of a General Force Field. *Journal of Physical Chemistry B* 108:1255-1266, 2004.

[15] Toukan, K., Rahman, A. Molecular-dynamics study of atomic motions in water. *Phys. Rev. B* 31(5):2643-2648, 1985.

[16] Cornell, W.; Cieplak, P.; et al. A Second Generation Force Field for the Simulation of Proteins, Nucleic Acids, and Organic Molecules. *Journal of the American Chemical Society* 117:5179-5197, 1995.

[17] Humphrey, W.; Dalke, A.; Schulten, K. VMD - Visual Molecular Dynamics. *Journal of Molecular Graphics* 14:33-38, 1996.

[18] Li, W.; Harrington, R.; et al. Differential Pair Distribution Function Study of the Structure of Arsenate Adsorbed on Nanocrystalline γ-Alumina. *Environmental Science and Technology* 45(22):9687-9692, 2011.

[19] Moroz, É.; Zyuzin, D.; et al. Radial Distribution Model Curves of Electron Density for Aluminum Oxides and Hydroxides. *Journal of Structural Chemistry* 48(4):704-707, 2007.

[20] Li, Y.; Gu, N. Thermodynamics of Charged Nanoparticle Adsorption on Charge-Neutral Membranes. *Journal of Physical Chemistry* 114, 2010.

[21] Johnston, C.; Chrysochoou, M. Mechanisms of chromate adsorption on hematite. *Geochimica et Cosmochimica Acta* 138:146-157, 2014.

[22] Samaraweera, M.; Jolin, W.; et al. Atomistic Prediction of Sorption Free Energies of Cationic Aromatic Amines on Montmorillonite: A Linear Interaction Energy Method. *Environmental Science and Technology Letters* 1:284-289, 2014.

[23] Parfitt, R.; Fraser, A.; et al. Adsorption on Hydrous Oxides II. Oxalate, Benzoate and Phosphate on Gibbsite. *Journal of Soil Science* 28(1):40-47, 1977.

[24] Parfitt, R.; Fraser, A.; et al. Adsorption on Hydrous Oxides III. Fulvic Acid and Humic Acid on Goethite, Gibbsite and Imogolite. *Journal of Soil Science* 28(2):289-296, 1977.

[25] Hung, K.; McBride, M. Adsorption of Para-substituted Benzoates on Iron Oxides. *Soil Science Society* 53:1673-1678, 1989.

[26] Oliviera, A.; Ladiera, A.; et al. Structrual model of As(III) adsorbed on gibbsite based on DFT calculations. *Journal of Molecular Structure: THEOCHEM* 762:17-23, 2006.

[27] Carrasquillo, A.; Bruland, G.; et al. Sorption of Ciprofloxacin and Oxytetracycline Zwitterions to Soils and Soil Minerals: Influence of Compound Structure. *Environmental Science and Technology* 42:7364-7642, 2008.

[28] Frisch, M.; Trucks, G.; et al. *Gaussian 09* Gauusian, inc.: Wallingford, CT, 2009.

[29] Bayly, C.; Cieplak, P.; et al. A Well-Behaved Electrostatic Potential Based Method Using Charge Restraints for Deriving Atomic Charges: The RESP Model. *Journal of Physical Chemistry* 97:10269-10280, 1993.

[30] Goldberg, S. Inconsistency in the triple layer model description of ionic strength dependent boron adsorption. *Journal of Colloid and Interface Science* 285(2):509-517, 2005.

[31] Kerisit, S.; Ilton, E.; et al. Molecular Dynamics Simulations of Electrolyte Solutions at the (100) Goethite Surface. *Journal of Physical Chemistry B* 110(41):20491-20501, 2006.

[32] Zukoski, C.; Saville, D. The interpretation of electrokinetic measurements using a dynamic model of the stern layer: II. Comparisons between theory and experiment. *Journal of Colloid and Interface Science* 114:45-53, 1986.

[33] Leroy, P.; Revil, A. A triple-layer model of the surface electrochemical properties of clay minerals. *Journal of Colloid and Interface Science* 270(2):371-380, 2004.